Dynamic Analysis of Capacitive Micromachined Ultrasonic Transducers

Baris Bayram, Goksen G. Yaralioglu, *Member, IEEE*, Mario Kupnik, A. Sanli Ergun, *Member, IEEE*, Ömer Oralkan, *Senior Member, IEEE*, Amin Nikoozadeh, and Butrus T. Khuri-Yakub, *Fellow, IEEE*

***Abstract*—Electrostatic transducers are usually operated under a DC bias below their collapse voltage. The same scheme has been adopted for capacitive micromachined ultrasonic transducers (cMUTs). DC bias deflects the cMUT membranes toward the substrate, so that their centers are free to move during both receive and transmit operations. In this paper, we present time-domain, finite element calculations for cMUTs using LS-DYNA, a commercially available finite element package. In addition to this DC bias mode, other new cMUT operations (collapse and collapse-snapback) have recently been demonstrated. Because cMUT membranes make contact with the substrate in these new operations, modeling of these cMUTs should include contact analysis. Our model was a cMUT transducer consisting of many hexagonal membranes; because it was symmetrical, we modeled only one-sixth of a hexagonal cell loaded with a fluid medium. The finite element results for both conventional and collapse modes were compared to measurements made by an optical interferometer; a good match was observed. Thus, the model is useful for designing cMUTs that operate in regimes where membranes make contact with the substrate.**

I. Introduction

CAPACITIVE micromachined ultrasonic transducers (cMUTs) were developed as an alternative to piezoelectric transducers [1]–[6]. cMUTs are usually operated under a DC bias, where the DC electrostatic forces attract the membrane toward the substrate to a point where the total electrostatic force is balanced by the stiffness of the membrane. When the bias voltage is increased beyond the point where the electrostatic forces can be restored by the mechanical stiffness, a structure under an electrostatic field collapses against the counter electrode. After collapse, the shape of the structure, and therefore the resonance frequency, changes significantly. When the bias voltage of a cMUT membrane is lower than the collapse voltage, the membrane deflects toward the substrate.

During normal operation, the center portion vibrates freely; if the collapse voltage is exceeded, the membrane collapses on to the substrate and the center of the membrane no longer moves. In this mode, the vibrating structure becomes an annular ring between the center and the rim of the membrane [7]. After collapse, the membrane is released from the substrate at a lower voltage than the collapse voltage. This voltage, termed snapback voltage, is determined by the relative dielectric constants of the membrane and the insulation layer. If relatively large AC excitation is applied [8], the membrane can also be biased for continuous operation between the collapse and snapback voltages (termed collapse-snapback).

As explained above, the bias voltage determines the operation regime of the cMUT. The bias voltage is generally kept below the collapse voltage of the membrane, so that the membrane does not go into the collapse region. Both static and dynamic models have been developed for this operation regime. Static models were used both to determine various membrane parameters such as collapse voltage and coupling coefficient [9], and to optimize the electrode size and position with respect to the membrane [10]. Lohfink *et al.*, developed linear and nonlinear models to evaluate the output pressure of a cMUT [11]. Linearized models, used to investigate the crosstalk between the membranes through harmonic and time domain analysis [12], revealed two main sources of coupling: a Scholte wave propagating at the transducer-fluid interface, and Lamb wave propagating in the substrate.

Nonlinear time domain finite element codes have also been developed for the modeling of cMUTs. In order to determine important considerations for the design of the cMUT, these models used either commercial finite element analysis (FEA) packages such as ANSYS (ANSYS Inc., Canonsburg, PA) [11] and PZFLEX (Weidlinger Associates Inc., Los Altos, CA) [13], [14], or developed their own FEA packages [15]–[18]. For example, the nonlinearity of the membrane motion was investigated in a 2D model using a single circular membrane [11]. In a 3D nonlinear time domain explicit finite element analysis, crosstalk between 1D array elements was investigated [13], and the effect of backing material on which substrate rests was reported in [14]. These finite element calculations all focused on understanding the cMUT dynamics in conventional operation regime. In order to develop models for the cMUTs operating in regimes where the membrane makes contact with the substrate, contact analysis must be included in the calculation. This paper presents the results obtained with a commercially available finite element method (FEM) package, LS-DYNA (LS-DYNA 970, Livermore Software Technology Corporation, Livermore, CA), and compares those calculations with experimental results

Manuscript received August 2, 2004; accepted April 20, 2005. This work was supported by the Office of Naval Research. M. Kupnik acknowledges the FWF Austrian Science Fund for financial support.

The authors are with the Edward L. Ginzton Laboratory, Stanford University, Stanford, CA 94305-4088 (e-mail: bbayram@stanford.edu).

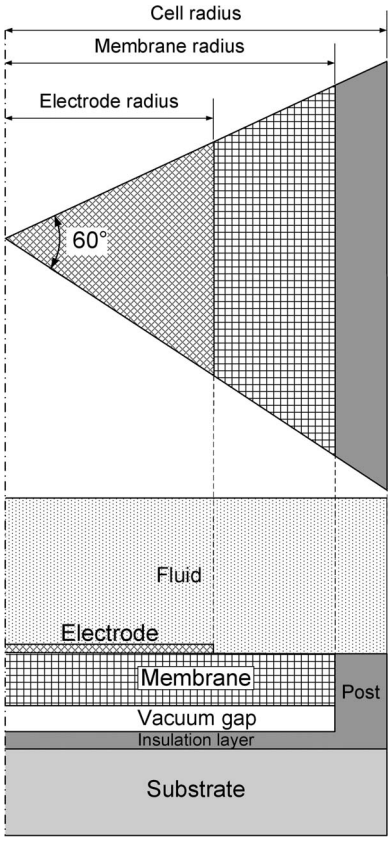

Fig. 1. The top and side views of the cMUT model. One-sixth of a hexagonal cell is modeled.

for a cMUT operating in both conventional and collapse mode.

II. Finite Element Analysis

In this study, a hexagonal membrane shape was used as the unit cell to cover the transducer area. The silicon nitride membrane was supported on the edges with silicon nitride posts (Fig. 1), with a vacuum gap between the membrane and the substrate. A thin insulation layer of silicon nitride over the highly doped silicon substrate prevented shorting in collapse by the ground electrode and the electrode on the membrane.

The cMUT was analyzed using a commercially available FEM package (LS-DYNA) [19]. The cMUT model is shown schematically in Fig. 1. Because the hexagonal cell was symmetrical, we modeled only one-sixth of the cell. In order to simulate an infinitely large cMUT composed of hexagonal membranes, symmetry boundary conditions were applied to the planes normal to the edges of the cell. The impedance-matched medium for the substrate was modeled by the absorbing boundary on the bottom of the substrate. The absorbing boundary was activated by the nonreflecting boundary specification in LS-DYNA [19].

The top of the membrane was covered with fluid to provide the acoustic medium for the wave propagation. The ground electrode was located beneath the insulation layer, and the other electrode was positioned on the top surface of the membrane. The electrodes were assumed to be infinitesimally thin. Contact elements were defined between the bottom surface of the membrane and the top surface of the insulation layer; sufficiently high voltages would collapse the membrane onto the insulation layer. While ideal contact (no friction and binding forces [19], [20]) was assumed in our model, extensive contact models and features are supported in LS-DYNA [19], [20].

TABLE I
Material Properties Used in Finite Element Analysis.

	Si	Si_3N_4	Soybean oil	Vacuum
Young's modulus (GPa)	169	320		
Density (kg/m^3)	2332	3270	930	
Poisson's ratio	0.29	0.263		
Relative permittivity		5.7		1
Velocity of sound (m/s)			1485	

Prior to the dynamic analysis, the cMUT was biased at a specific voltage, and atmospheric pressure was included in the calculations. In order to bias the cMUT in the collapse operation regime, two voltages were applied consecutively: the first was higher than the collapse voltage; the second was the actual bias voltage.

Because the contact behavior was assumed to be ideal (without friction), residual stress in the membrane was not included in this analysis. A linear wave equation was used to describe the propagation of the acoustic wave in the immersion fluid.

LS-DYNA does not have a coupled field solver for electrostatic and structural analysis, but it includes a subroutine to define loads (user loading function) as a function of displacements [19]. After the subroutine for electrostatic force calculation was developed, the source file was compiled with the LS-DYNA object files, using Compaq Visual Fortran Compiler 6.6B (HP-Compaq, Palo Alto, CA). The object files were provided by Livermore Software Technology Corporation (LSTC).

The mechanical and electrical material properties used in the FEM calculations are given in Table I. The only material parameter required for the electrostatic analysis was the dielectric constant. The structural analysis used Young's modulus, density, and Poisson's ratio for the solids; density and sound velocity were used for the fluid acoustic medium.

III. Experiments

In the experiments, the cMUT was immersed in oil, with the top surface parallel to the air-oil interface [Fig. 2(a)]. The physical parameters of the cMUT [Fig. 2(b)] used in all experiments described in this work are listed in Table II. The active area was 86% of the total 7-mm × 7-mm transducer area. An optical interferometer was used to measure the displacement of the air-oil interface.

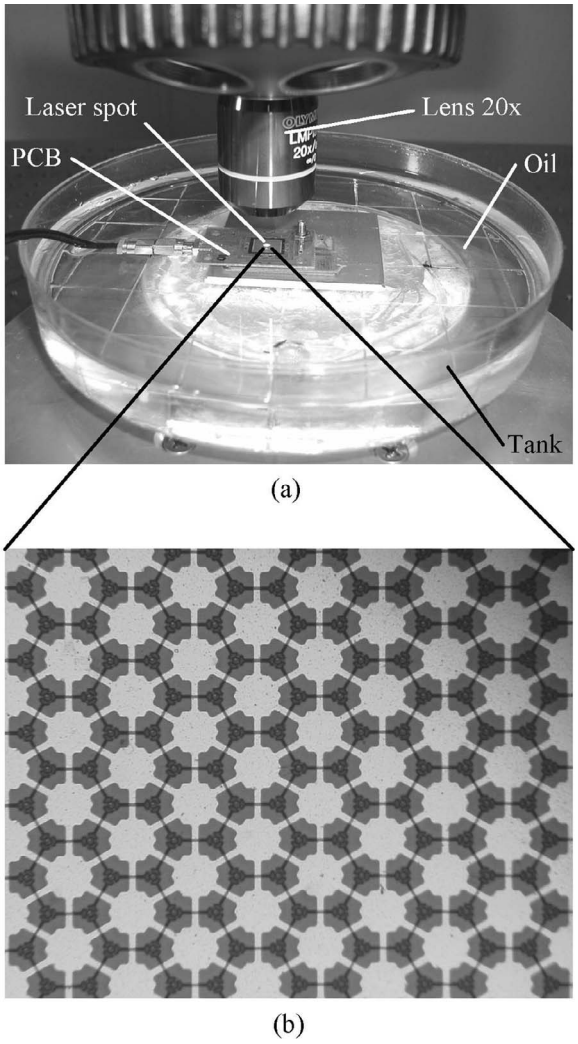

Fig. 2. (a) Photographs of the cMUT mounted on a printed circuit board (PCB), immersed in oil; the cMUT is under the microscope, which is connected to an optical interferometer. (b) Zoomed top view of some cMUT cells (see Table II for the dimensions).

TABLE II
PHYSICAL DIMENSIONS OF THE CMUT (ALL IN μM).

Cell radius	43
Membrane radius	40
Electrode radius	25
Membrane thickness	1
Vacuum gap	0.65
Insulation thickness	0.2
Substrate thickness	500

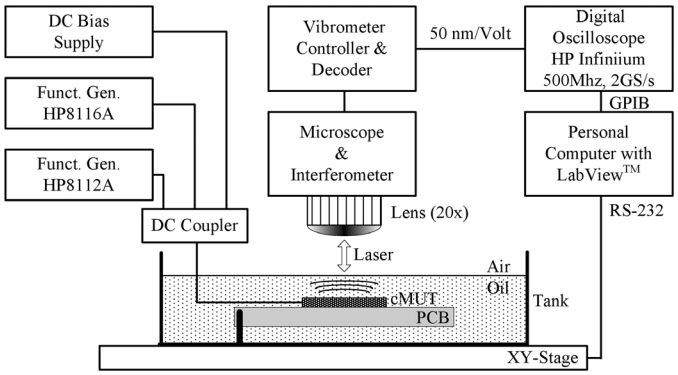

Fig. 3. Overview of the experimental setup with all components, consisting of an immersed cMUT mounted on a PCB. An optical interferometer, connected to a microscope, was used to measure both the membrane displacement and the oil-air interface displacement. Two function generators were used to generate the bipolar pulse.

The experimental setup (Fig. 3) consisted of an optical fiber interferometer OFV-511 (Polytec GmbH, Waldbronn, Germany) attached to a common microscope by a microscope adapter OFV-072 (Polytec). The interferometer was connected to an ultrasonics vibrometer controller OFV-2700/2 (Polytec) that contains a modified wide-band displacement decoder OVD-30 (Polytec) with an extended frequency range. Thus, the system offered a frequency range from 50 kHz to 30 MHz, and was able to detect amplitudes in the subnanometer range. The specified displacement range for this system was $\pm$75 nm for frequencies from 50 kHz to 20 MHz, and $\pm$50 nm for frequencies from 20 MHz to 30 MHz. The system also enabled the acquisition of transient pulses, deemed essential for this work. The output level was 50 nm per volt with 50 Ω termination. The calibration error was specified with $< \pm 3\%$ at 100 kHz/50 $\mathrm{nm_{p\text{-}p}}$.

A digital oscilloscope (Infiniium 500 MHz, 2GS/s, Agilent Technologies Inc., Palo Alto, CA) was used to calculate the output of the interferometer decoder; the data were transferred over a GPIB—IEEE 488 bus to a common personal computer (PC). LabView^{TM} Version 6.0 (National Instruments, Austin, TX) software was used to control an xy-stage, which allowed the entire oil tank to be moved under the lens (20$\times$ and 100$\times$, respectively) of the microscope with μm-resolution. The 100$\times$ lens was used primarily to adjust the cMUT alignment.

Only the transmitting mode of the cMUT was used for the experiments described in this work: i.e., the cMUT was driven by a DC voltage (up to 160 V) with a superimposed AC signal (bipolar pulse, generated by two pulse/function generators HP8116A and HP8112A, Agilent Technologies Inc.) that was supplied through a DC coupler (Fig. 3). The burst rate was set to 100 Hz.

To avoid measuring signals caused by ultrasonic waves reflected between the cMUT and the oil-air interface, the distance from the cMUT to the air-oil interface was set to 2.25 mm.

IV. RESULTS

A. Conventional Mode of Operation

The cMUT with the physical dimensions given in Table II was biased at 130 V; for conventional operation, one cycle of 1 MHz bipolar pulse (-7 V, 500-ns pulse, followed by $+7$ V, 500-ns pulse) was applied at $t = 0$ μs.

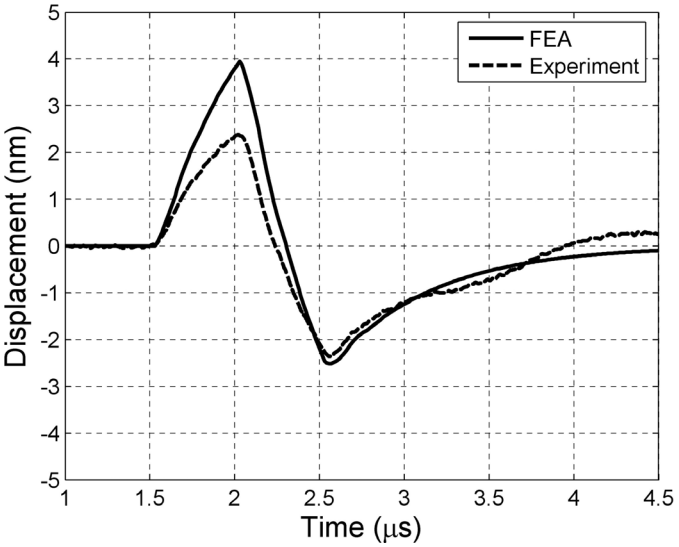

Fig. 4. The displacement of the cMUT in the conventional mode of operation. The solid and dashed lines represent the FEA and the experiment, respectively.

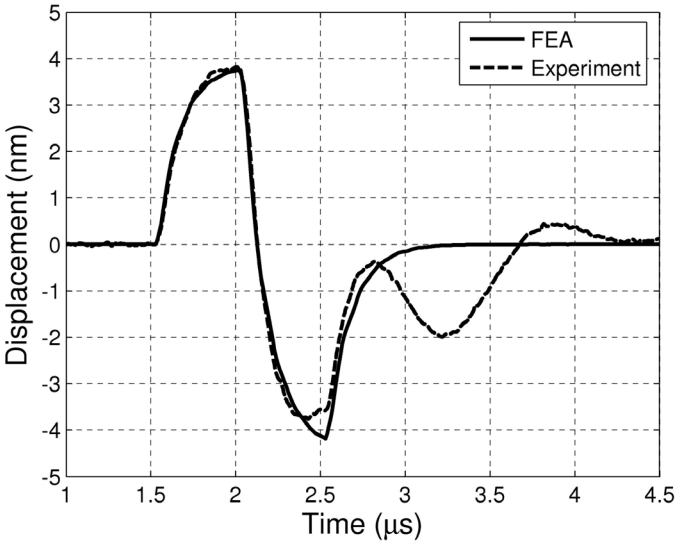

Fig. 5. The displacement of the cMUT in collapse mode of operation. The solid and dashed lines represent the FEA and the experiment, respectively.

The ultrasonic waves from the cMUT surface reached the air-oil interface at $t = 1.5$ μs. The output displacements of the cMUT from both the FEA and the experiment are depicted in Fig. 4. The displacement of the air-oil interface was divided by two to take the interface reflection into account. During the first negative pulse, the membrane displacement increased in the positive direction. In both the FEA and the experiment, peak displacements of 3.8 nm and 2.4 nm were achieved at $t = 2.0$ μs, respectively. A subsequent positive pulse decreased the membrane displacement. The peak displacement of -2.3 nm, achieved at $t = 2.5$ μs in both FEA and experiment, gradually reached zero displacement at $t = 4.5$ μs.

B. Collapse Mode of Operation

The same cMUT was biased at 160 V in collapse; the same bipolar pulse was applied in collapse operation. The output displacements of the cMUT from both the FEA and the experiment are depicted in Fig. 5. During the first negative pulse, the membrane displacement increased in the positive direction. In both the FEA and the experiment, peak displacements of 3.7 nm and 3.8 nm were achieved at $t = 2.0$ μs, respectively. A subsequent positive pulse decreased the membrane displacement. The peak displacement of -4.0 nm, achieved at $t = 2.5$ μs in FEA, gradually reached zero displacement at $t = 3.2$ μs. In the experiment, a low frequency wave, not predicted by the FEA, was observed after $t = 2.8$ μs.

V. Discussion

Time-domain finite element packages use either implicit (ANSYS) or explicit (PZFLEX, LS-DYNA) time integration methods. Implicit methods result in unconditional stability in linear problems, and large time steps can be used in the calculations. However, implicit methods become unstable for highly nonlinear contact problems.

While explicit methods are stable even for highly nonlinear situations, the stability requires that very small time steps be used in each calculation. The size of the time step is bounded by the largest natural frequency of the structure, which, in turn, is bounded by the highest frequency of any individual element in the finite element mesh [18]. The uncoupled equation sets in the explicit method allow a faster solution for each time step calculation; computation time scales almost linearly with the number of elements in the model. Because implicit methods, due to the solution of the coupled equation sets, are impractical, explicit methods dominate the time-domain, nonlinear analysis of very large models. We chose LS-DYNA for the finite element calculation for its enhanced contact capabilities and explicit time domain solver.

In Figs. 4 and 5, the FEA and the experimental membrane displacements showed similar time responses. In collapse operation, the FEA and the experiment differed by less than 5% during the pulse excitation. A noticeable difference between the FEA and the experiment (Fig. 5) is the presence of a strong wave after $t = 2.8$ μs, which was not predicted by FEA. While a central assumption in FEA is the infinite dimensions of the cMUT, in this experiment, a 7-mm $\times$ 7-mm cMUT was used. The finite dimensions of the cMUT caused lateral waves reflecting back and forth from the edges. These reflections were calculated to reach the air-oil interface at $t = 2.8$ μs, as observed in the experiment. Therefore, the time response of the cMUT from $t = 1.5$ μs up to $t = 2.8$ μs in the experiment was not affected by the finite dimensions of the transducer. The good match between the FEA and the experiment in this time interval verified the validity of the results obtained by LS-DYNA.

The FEA overestimated the peak displacement at $t = 2.0$ μs in conventional operation (Fig. 4), compared to experimental results. This mismatch is currently under investigation to determine its origin.

VI. Conclusions

The time-domain, finite element calculations were performed using a commercially available FEM package, LS-DYNA. The finite element calculations for conventional and collapse modes were compared to experimental results obtained via interferometer. Good match between FEA and experiment was observed in time-domain response of the cMUT. LS-DYNA was used for the first time to model cMUTs in this study. The model is useful for designing cMUTs operating in new regimes where membranes make contact with the substrate.

Acknowledgments

The authors thank Wayne L. Mindle and Khanh Bui from Livermore Software Technology Corporation (LSTC) for providing technical assistance in LS-DYNA and object files for user-defined loading implementation, and Scott Rodamaker from MCR Associates, Inc., for providing technical support in ANSYS and ANSYS/LS-DYNA.

References

[1] M. I. Haller and B. T. Khuri-Yakub, "A surface micromachined electrostatic ultrasonic air transducer," in *Proc. IEEE Ultrason. Symp.*, 1994, pp. 1241–1244.

[2] P.-C. Eccardt, K. Niederer, T. Scheiter, and C. Hierold, "Surface micromachined ultrasound transducers in CMOS technology," in *Proc. IEEE Ultrason. Symp.*, 1996, pp. 959–962.

[3] I. Ladabaum, X. Jin, H. T. Soh, A. Atalar, and B. T. Khuri-Yakub, "Surface micromachined capacitive ultrasonic transducers," *IEEE Trans. Ultrason., Ferroelect., Freq. Contr.*, vol. 45, no. 3, pp. 678–690, May 1998.

[4] Ö. Oralkan, A. S. Ergun, J. A. Johnson, M. Karaman, U. Demirci, K. Kaviani, T. H. Lee, and B. T. Khuri-Yakub, "Capacitive micromachined ultrasonic transducers: Next-generation arrays for acoustic imaging?," *IEEE Trans. Ultrason., Ferroelect., Freq. Contr.*, vol. 49, no. 11, pp. 1596–1610, Nov. 2002.

[5] O. Ahrens, A. Buhrdorf, D. Hohlfeld, L. Tebje, and J. Binder, "Fabrication of gap-optimized CMUT," *IEEE Trans. Ultrason., Ferroelect., Freq. Contr.*, vol. 49, no. 9, pp. 1321–1329, Sep. 2002.

[6] G. Caliano, R. Carotenuto, A. Caronti, and M. Pappalardo, "cMUT echographic probes: Design and fabrication process," in *Proc. IEEE Ultrason. Symp.*, 2002, pp. 1067–1070.

[7] B. Bayram, E. Hæggström, G. G. Yaralioglu, and B. T. Khuri-Yakub, "A new regime for operating capacitive micromachined ultrasonic transducers," *IEEE Trans. Ultrason., Ferroelect., Freq. Contr.*, vol. 50, no. 9, pp. 1184–1190, Sep. 2003.

[8] B. Bayram, Ö. Oralkan, A. S. Ergun, E. Hæggström, G. G. Yaralioglu, and B. T. Khuri-Yakub, "Capacitive micromachined ultrasonic transducer design for high power transmission," *IEEE Trans. Ultrason., Ferroelect., Freq. Contr.*, vol. 52, no. 2, pp. 326–339, Feb. 2005.

[9] G. G. Yaralioglu, A. S. Ergun, B. Bayram, E. Hæggström, and B. T. Khuri-Yakub, "Calculation and measurement of electromechanical coupling coefficient of capacitive micromachined ultrasonic transducers," *IEEE Trans. Ultrason., Ferroelect., Freq. Contr.*, vol. 50, no. 4, pp. 449–456, Apr. 2003.

[10] A. Bozkurt, A. Atalar, and B. T. Khuri-Yakub, "Theory and analysis of electrode size optimization for capacitive microfabricated ultrasonic transducers," *IEEE Trans. Ultrason., Ferroelect., Freq. Contr.*, vol. 46, no. 6, pp. 1364–1374, Nov. 1999.

[11] A. Lohfink, P. C. Eccardt, W. Benecke, and H. Meixner, "Derivation of a 1D CMUT model from FEM results for linear and nonlinear equivalent circuit simulation," in *Proc. IEEE Ultrason. Symp.*, 2003, pp. 465–468.

[12] Y. Roh and B. T. Khuri-Yakub, "Finite element analysis of underwater capacitor micromachined ultrasonic transducers," *IEEE Trans. Ultrason., Ferroelect., Freq. Contr.*, vol. 49, no. 3, pp. 293–298, Mar. 2002.

[13] G. Wojcik, J. Mould, P. Reynolds, A. Fitzgerald, P. Wagner, and I. Ladabaum, "Time-domain models of MUT array cross-talk in silicon substrates," in *Proc. IEEE Ultrason. Symp.*, 2000, pp. 909–914.

[14] I. Ladabaum, P. Wagner, C. Zanelli, J. Mould, P. Reynolds, and G. Wojcik, "Silicon substrate ringing in microfabricated ultrasonic transducers," in *Proc. IEEE Ultrason. Symp.*, 2000, pp. 943–946.

[15] M. Kaltenbacher, H. Landes, S. Reitzinger, and R. Peipp, "3-D simulation of electrostatic-mechanical transducers using algebraic multigrid," *IEEE Trans. Magn.*, vol. 38, no. 2, pp. 985–988, Mar. 2002.

[16] E. Zhelezina, M. Kaltenbacher, and R. Lerch, "Numerical simulation of acoustic wave propagation by a time and space adaptive finite element method," in *Proc. IEEE Ultrason. Symp.*, 2002, pp. 1213–1216.

[17] M. Kaltenbacher, H. Landes, K. Niederer, and R. Lerch, "3D simulation of controlled micromachined capacitive ultrasound transducers," in *Proc. IEEE Ultrason. Symp.*, 1999, pp. 1155–1158.

[18] K. Niederer, P. C. Eccardt, H. Meixner, and R. Lerch, "Micromachined transducer design for minimized generation of surface waves," in *Proc. IEEE Ultrason. Symp.*, 1999, pp. 1137–1139.

[19] LS-DYNA 970 Keyword User's Manual, Livermore Software Technology Corporation, Livermore, CA, 2003.

[20] LS-DYNA 970 Theoretical Manual, Livermore Software Technology Corporation, Livermore, CA, 2003.

Baris Bayram was born in Izmir, Turkey. He received the B.S. degree in 2000 from Bilkent University, Turkey, the M.S. degree in 2002 from Stanford University, both in electrical engineering. He is currently a Ph.D. candidate in electrical engineering at the E. L. Ginzton Laboratory of Stanford University. His current research interests include the accurate modeling of capacitive micromachined ultrasonic transducers (cMUTs) using static and dynamic FEM. He particularly investigates the nonlinear operation regimes (collapse and collapse-snapback) of cMUTs for high performance. He is a member of the IEEE.

Goksen Goksenin Yaralioglu (S'92–M'99) was born in Akhisar, Turkey, on May 13, 1970. He received his B.S., M.S., and Ph.D. degrees from Bilkent University, Turkey, in 1992, 1994, and 1999, respectively, all in electrical engineering. He is now working as an engineering research associate in E. L. Ginzton Laboratory, Stanford University. His current research interests include design, modeling and applications of micromachined ultrasonic transducers, and atomic force microscopy at ultrasonic frequencies.

Mario Kupnik was born in Leoben, Austria, in 1974. He received his M.S. in electronics engineering from the Graz University of Technology, Graz, Austria, in 2000. From summer 1999 to October 2000, he worked as an Analog Design Engineer for Infineon Technologies AG, Graz, Austria, on the design of ferroelectric memories and contactless smart card systems.

From 2000 to 2004, Dr. Kupnik worked as a research assistant at the Christian-Doppler Laboratory for Sensory Measurement, c/o Institute for Automation, University of Leoben, Austria. He received his Ph.D. in Physical Measurement Techniques from the University of Leoben in 2004 for his research in ultrasonic flow metering of hot gaseous mixtures, focusing especially on the exhaust gases of automotive combustion engines.

He is currently a post-doctoral researcher in the Khuri-Yakub Ultrasonics Group at the E. L. Ginzton Laboratory at Stanford University. His research interests include the design and application of capacitive micromachined ultrasonic transducers, focusing especially on ultrasonic transit-time gas flowmeters for hot and pulsating gases, and on ultrasonic nondestructive evaluation. Dr. Kupnik received the 2004 Fred-Margulies Award of the International Federation of Automatic Control (IFAC). He holds four patents in the fields of analog front-end circuits for contactless smart card systems and ultrasonic transit-time gas flowmeters.

Arif Sanli Ergun (S'91–M'99) was born in Ankara, Turkey, in 1969. He received his B.Sc., M.Sc., and Ph.D. degrees in 1991, 1994, and 1999, respectively, all in electrical and electronics engineering from Bilkent University, Turkey. He is now at the E. L. Ginzton Laboratory, Stanford University, as an engineering research associate. His main research interests are acoustics, ultrasound, microelectromechanical systems (MEMS), and microwave electronics.

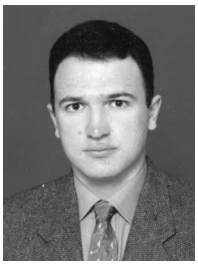

Ömer Oralkan (S'93) was born in Izmit, Turkey, in 1973. He received a B.S. degree from Bilkent University, Ankara, Turkey, in 1995, an M.S. degree from Clemson University, Clemson, SC, in 1997, and a Ph.D. degree from Stanford University, Stanford, CA, in 2004, all in electrical engineering.

From 1995 to 1996, he was a hardware and network engineer at Bilkent University Computer Center, Ankara, Turkey. In the summer of 1997, he worked as a process engineer at the National Semiconductor Research Laboratories, Santa Clara, CA. Currently, he is an engineering research associate at the Edward L. Ginzton Laboratory at Stanford University. His past and present research interests include analog and digital circuit design, micromachined sensors and actuators, and semiconductor device physics and fabrication. His current research focuses on the design and implementation of integrated ultrasonic imaging systems.

He is a co-recipient of the Best Paper Award presented at the IEEE International Symposium on the Physical and Failure Analysis (IPFA). He also received the 2002 Outstanding Paper Award of the IEEE Ultrasonics, Ferroelectrics, and Frequency Control Society. Dr. Oralkan is a member of the IEEE.

Amin Nikoozadeh received his B.S. from Sharif University of Technology, Tehran, Iran, in 2002 and his M.S. from Stanford University, Stanford, CA, in 2004, both in electrical engineering. He is currently pursuing his Ph.D. in electrical engineering at Stanford. Mr. Nikoozadeh's research interests include analog and mixed-signal VLSI data converters, and modeling, design, and implementation of integrated ultrasonic imaging systems.

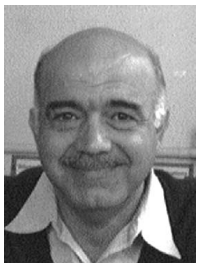

Butrus T. Khuri-Yakub (S'70–S'73–M'76–SM'87–F'95) was born in Beirut, Lebanon. He received the B.S. degree in 1970 from the American University of Beirut, the M.S. degree in 1972 from Dartmouth College, and the Ph.D. degree in 1975 from Stanford University, all in electrical engineering. He joined the research staff at the E. L. Ginzton Laboratory of Stanford University in 1976 as a research associate. He was promoted to senior research associate in 1978, and to a Professor of Electrical Engineering (Research) in 1982. He has served on many university committees in the School of Engineering and the Department of Electrical Engineering.

Presently, he is the Deputy Director of the E. L. Ginzton Laboratory, and the associate chairman for graduate admissions in the electrical engineering department at Stanford. Professor Khuri-Yakub has been teaching both at the graduate and undergraduate levels for over 20 years, and his current research interests include in situ acoustic sensors (temperature, film thickness, resist cure, etc.) for monitoring and control of integrated circuits manufacturing processes, micromachining silicon to make acoustic materials and devices such as airborne and water immersion ultrasonic transducers and arrays, and fluid ejectors, and in the field of ultrasonic nondestructive evaluation and acoustic imaging and microscopy.

Professor Khuri-Yakub is a fellow of the IEEE, a senior member of the Acoustical Society of America, and a member of Tau Beta Pi. He is associate editor of Research in Nondestructive Evaluation, a Journal of the American Society for Nondestructive Testing. Professor Khuri-Yakub has authored over 400 publications and has been principal inventor or co-inventor of 60 issued patents. He received the Stanford University School of Engineering Distinguished Advisor Award, June 1987, and the Medal of the City of Bordeaux for contributions to NDE, 1983.